Proceedings of the ASME/BATH 2023
Symposium on Fluid Power and Motion Control
FPMC2023
October 16-18, 2023, Sarasota, United States

FPMC2023-111819

HUMAN-IN-THE-LOOP MOTION CONTROL OF A TWO-DOF HYDRAULIC BACKHOE POWERED BY THE HYBRID HYDRAULIC ELECTRIC ARCHITECTURE (HHEA)

Arpan Chatterjee and Perry Y. Li*
Department of Mechanical Engineering
The University of Minnesota
Minneapolis, Minnesota 55455
Email: {chatt116,lixxx099}@umn.edu

ABSTRACT

The Hybrid Hydraulic-Electric Architecture (HHEA) combines the respective power density and control advantages of hydraulic and electric actuation to save energy for off-road vehicles. It uses a set of selectable common pressure rails to transmit the majority of power and electric actuation to modulate that power. As it is critical that off-road vehicles can perform tasks dexterously and exactly as commanded by the operator, the switchings between discrete pressure rails pose a potential challenge for smooth and precise motion. A control strategy consisting of a backstepping nominal control and least norm transition control has previously been developed to address this issue. It has been tested on 1 degree of freedom (DOF) testbeds where known trajectories were able to be tracked precisely. This paper presents the implementation of the HHEA motion control strategy on a 2-DOF backhoe operated by a human operator via a 2-DOF joystick. Unlike previous studies, the duty cycle is unknown beforehand and the decision to change pressure rails is taken in real-time. The efficacy of the motion control strategy has been validated experimentally. Several strategies to improve the user interface: control in workspace coordinates, pressure feedback, and velocity field-based task specification, have also been implemented and demonstrated to make operating the multiple DOF, HHEA actuated machine more intuitive to novice operators.

*Corresponding author.

1 INTRODUCTION

Conventional off-highway vehicles utilized in the construction and agriculture rely on hydraulic actuation to power multiple degrees of freedom. However, these machines are quite inefficient and consume significant amount of energy [1]. By making them more energy efficient, CO_2 emissions as well as operating costs can be reduced. This is beneficial both to the environment and financially.

In the quest for increasing the efficiency of conventional off-highway vehicles used in construction and agriculture, Li et al. [2] have proposed the Hybrid Hydraulic-Electric Architecture (HHEA). This architecture combines the power density advantage of hydraulic systems with the efficiency and controllability benefits offered by electric actuation. The HHEA, illustrated in Figure 1, incorporates a set of common pressure rails (CPRs) and an electric motor-driven pump/motor to manage each degree of freedom. By utilizing the electric motor drive, the HHEA allows for direct control of flow and, consequently, actuator speed. The system strategically selects a pair of pressure rails for the pump/motor inlet (P_B) and the return port of the hydraulic actuator (P_A) to deliver hydraulic force close to the desired actuator force. This arrangement minimizes the electric motor's responsibility to only compensate for any discrepancy, ensuring that the majority of power transmission occurs hydraulically, while the electric motors function primarily to modulate the power. This significantly reduces the torque and power requirements for the electric motors and hence the cost of electrification. Note that the HHEA is inherently throttle-less (as only switching on/off

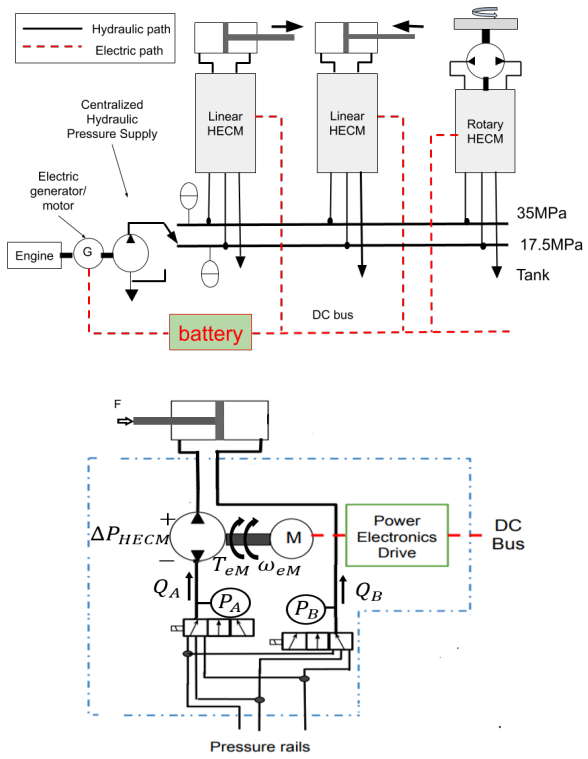

FIGURE 1. Top: The hybrid hydraulic-electric architecture (HHEA) with 3 services and 3 pressure rails at 0 MPa, 17.5 MPa, and 35 MPa. The electric generator/motor at the engine is optional. Bottom: Hydraulic-Electric Control Module (HECM) for a linear actuator.

valves are used), capable of capturing regenerative energy from the load. Previous studies have demonstrated 50% to 80% energy savings compared to baseline load sensing systems for the work circuits of various off-road mobile machines [2–4].

While prioritizing energy efficiency in off-road machines is undoubtedly crucial, it is equally vital that these machines can execute tasks precisely and accurately in response to given commands. This paper addresses the motion control aspect of the Hybrid Hydraulic-Electric Architecture (HHEA) in the presence of a human operator. The unique characteristic of the HHEA, which involves discrete pressure changes when transitioning between different sets of pressure rails for the pump/motor inlet and actuator port, presents a challenge for motion control. These pressure rail transitions are essential to maximize system efficiency or maintain the system within the torque capability of the electric motor. To address this challenge, a motion control strategy has been developed and successfully validated on 1-DOF hardware [5] [6]. The strategy consists of a passivity-based integral controller as a nominal controller, employed during periods of consecutive pressure rail transitions to ensure smooth operation, and a least norm feedforward controller as a transition controller, utilized for the brief duration when the pressure rails undergo discrete switching to manage the system's response during this critical period.

In this paper, we present the results for implementating the motion control strategy of HHEA on a 2-degree-of-freedom (DOF) backhoe arm operated by a human operator using a joystick. The boom and stick actuators of the backhoe arm have been retrofitted with HHEA, and a 2-degree-of-freedom joystick is employed to control the boom and stick motion. Whereas in previous studies [5–7], the duty cycle trajectory is known beforehand and the pressure rail switching decisions were made offline, in the present study, the duty cycle is provided by the human operator in real time and is unknown a priori. To account for this, a real-time pressure rail switching strategy is proposed which makes pressure rail switching decisions based on the present information of the load force. To further aid operators, especially novice operators, to perform useful tasks on the multi-DOF backhoe, a human-machine control strategy has also been developed to make operating the backhoe more intuitive. Three strategies have been proposed and tested: Cartesian work space control, pressure feedback, and using velocity field for specifying tasks. Each strategy provides an appropriate reference velocity that the low level real-time HHEA motion strategy executes.

The rest of the paper is organized as follows. Section 2 describes the HHEA and our motion control objectives with the architecture. The real-time rail switching strategy is presented in Section 3. The motion control strategy is presented in Section 4. The Human-in-the-loop test-bed along with motion control and rail switching results is presented in Section 5. Improvements to the human machine interface are presented in Section 6. Finally, Section 7 contains some concluding remarks.

2 System Description and Control Architecture

Figure 1 illustrates the HHEA with $N = 3$ common pressure rails (CPRs), at various nominal pressures $\{P_{R1}, \ldots, P_{RN}\}$. These rails are supplied by a common pump/motor, and the pressure at each rail is regulated by a hydraulic accumulator to maintain a constant value. For each degree-of-freedom (DOF), a hydraulic-electric control module (HECM) comprising an electric motor driven hydraulic pump/motor and a set of switching valves for selecting which pressure rails are connected. The HECM combines hydraulic power from the pressure rails with electric power to drive the linear degree-of-freedom (refer to Fig. 1-bottom).

To simplify the explanation, let us momentarily disregard pressure and inertia dynamics. Assuming the selected pressure rails with pressures P_{Ri} and P_{Rj} are connected to the inlet of the HECM pump/motor P_B and the hydraulic actuator return P_A, and the electric motor torque is T_m, the resulting actuator force F_{act}

and speed $\dot{x}$ can be expressed as follows:

$$F_{act} = P_{Ri}A_{cap} - (P_{Rj} + \frac{2\pi}{D}T_m)A_{rod}$$
$$= \underbrace{(P_{Ri}A_{cap} - P_{Rj}A_{rod})}_{Frail} - \underbrace{A_{rod}\frac{2\pi}{D}T}_{Felect} \quad (1)$$

$$\dot{x} = -\frac{D}{2\pi A_{rod}}\omega \quad (2)$$

Here, D represents the HECM pump/motor displacement, A_{cap} and A_{rod} are the areas of the cap and rod side pistons, and F_{rail} and F_{elect} denote the components of the actuator force provided by the selected pressure rails and the electric motor, respectively. The equation (1) reveals that there are potentially N^2 options for F_{rail} based on different combinations of pressure rail selections. Therefore, by choosing the pressure rails so that F_{rail} is close to the desired F_{act}, the electric motor torque can be minimized, allowing for downsizing of the electric motor.

In the presence of pressure and inertia dynamics, the system dynamics become:

$$M\ddot{x} = P_{cap}A_{cap} - P_{rod}A_{rod} - F_L - f \quad (3)$$

$$\dot{P}_{rod} = \frac{\beta}{V_{rod}(x)}(Q + A_{rod}\dot{x}) \quad (4)$$

$$Q = \frac{D}{2\pi}\omega \quad (5)$$

$$J\dot{\omega} = \frac{(P_B - P_{rod})D}{2\pi} + T_m \quad (6)$$

where $F_L(t)$ is the load on the actuator, $P_{cap} = P_A$ and P_{rod} are the actuator chamber pressures, f is the combination of viscous friction and stiction on the hydraulic cylinder, β is the bulk modulus of the fluid, $V_{rod}(x) := V_o - A_{rod}x$ is the rod side fluid volume, J is the inertia of the electric motor and the pump/motor, and P_B is the inlet pressure of the pump/motor. P_A (i.e. P_{cap}) and P_B are connected to the selected pressure rails so that $P_A,\ P_B \in \{P_{R1}, \ldots, P_{RN}\}$. Because these selections can change instantaneously, $P_B(t)$ and $P_{cap}(t)$ can undergo discrete jumps. In between rail transitions, P_B and P_{cap} are constant.

The HHEA uses a two-tiered controller design, consisting of a high-level and a low-level controller. The high-level controller's objective is to minimize system losses by selecting appropriate pressure rails (P_{Ri} and P_{Rj}) on both the cap and rod sides, given the limited torque availability. Meanwhile, the low-level controller is responsible for the motion control of the HHEA. The primary objective of the motion control for HHEA is to track a desired position or velocity reference trajectory set by the operator using the HECM's electric motor torque (T_M) as the control input. Two different controllers have been designed for two different operation zones. A nominal controller is designed for the duration between two pressure rail switches, and a transition controller is designed to handle pressure rail switches. The nominal controller is based on Passivity-based Backstepping Integral control, which ensures the robustness of the system while providing accurate tracking of reference trajectories. The transition controller, on the other hand, is based on Least Norm Control, which minimizes the control input required to achieve a desired final state during a pressure rail switch.

3 Real-time switching strategy

The Hybrid Hydraulic Electric Architecture relies heavily on efficient switching among the pressure rails to minimize the size of the electric components and maximize fuel savings. The high-level controller plays a critical role in selecting the pressure rails based on the system's performance and prior knowledge of the duty cycle and component operational zones. This requires the optimization process to be computed offline over the entire drive cycle [8]. However, future drive cycle information is unavailable when a human operator drives these mobile machines. Therefore, a real-time pressure rail switching strategy is necessary to drive the system with reduced electric component sizes.

To ensure efficient operation within the limits of the electric motor torque, the decision to switch among pressure rails is based on the load acting on the actuator. The actuator load force is estimated from the pressure measurements on both the cap and rod sides of the actuator as:

$$F_L(t) = P_c(t)A_c - P_r(t)A_r \quad (7)$$

where $P_c(t)$, $P_r(t)$ are the pressure measurements on the cap and rod side of the actuator and A_c, A_r are the cap and rod side areas respectively. The estimated load force is compared with each of the rail forces to determine the most suitable combination of pressure rails. Nominally, the cost function for choosing pressure rails is the absolute difference between the rail forces and the actuator load so that the selected rail force F_* is given as :

$$F_* = \arg\min_{F_R \in F_{Rails}} \left[Cost(F_R, F_L)\right] \quad (8)$$

$$Cost(F_R, F_L) := |F_R - F_L| \quad (9)$$

This choice of cost function aims to select the rail force that is closest to the actuator load so as to minimize electric force. The decision is assessed at each time step, except during a switching decision where it is evaluated after the switching period concludes.

However, if the chosen rail force leads to cavitation, the cost associated with that rail force is set to infinity, rendering it infeasible. In such cases, the optimization process identifies the

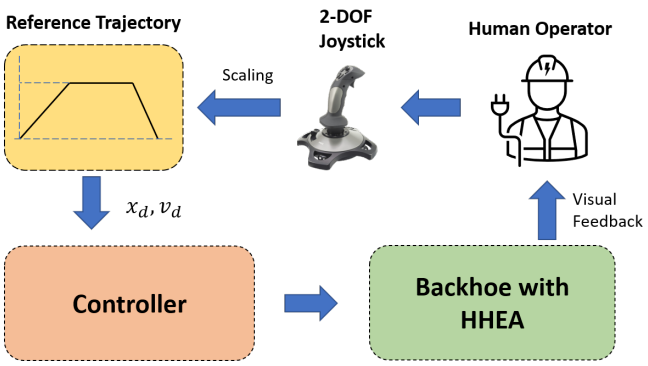

FIGURE 2. Backhoe control system

next best alternative. There is also a penalty function that gets added to the cost and it incentivizes the system to stay in the current pressure rail selections until sufficient time has passed or the cost difference becomes higher:

$$P_R = A(F_R, F_*)e^{-\lambda*(t-t_s)} \tag{10}$$

$$A(F_R, F_*) = 0 \; for \; F_R = F_* \tag{11}$$

Here, P_R is the penalty associated with F_R, and t_s is the last rail switching time. This penalty decreases exponentially with elapsed time since the last switch is only added to all the other rail selections that are currently not selected. It is important to note that this approach represents a sub-optimal solution since the decision to switch is based on minimizing the electric motor torque, rather than on the objective of minimizing losses in the system. In contrast, offline optimization using dynamic programming and lagrange multiplier methods [8,9] involves a more comprehensive analysis that considers a broader range of factors when making switching decisions, resulting in the identification of the optimal solution.

4 Reference Command and Tracking

The high-level human-in-loop control design is illustrated in Figure 2. In this setup, a human operator utilizes a 2-degree-of-freedom (DOF) joystick to establish the reference velocity for the stick and boom actuators of the backhoe arm. The position of the joystick is normalized and mapped to a corresponding set velocity reference. The maximum velocity reference is achieved when the joystick is in its maximum position. By dynamically adjusting the joystick position in real-time (from -1 to 1), the human operator can effectively set the desired velocity reference for the control system. The velocity is integrated to get the position reference. Both velocity and position reference is fed to the motion controller. The motion controller uses passivity-based integral backstepping control for nominal conditions when the pressure

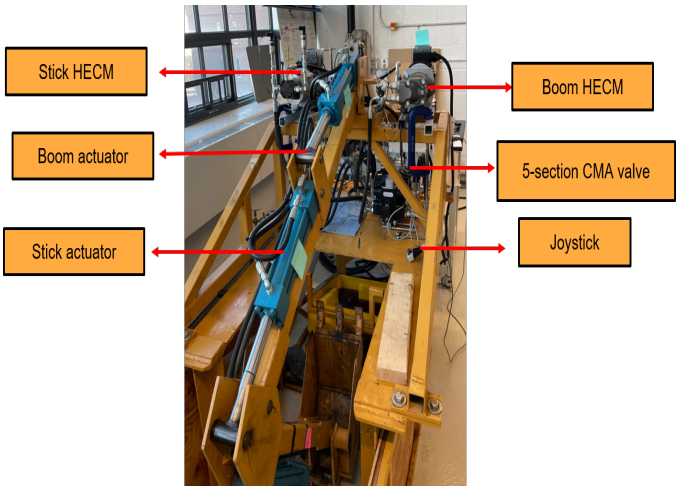

FIGURE 3. Backhoe testbed

rails are not switching and the Least Norm control is used as the transition controller when the pressure rail switches. The formulation and derivation of the nominal controller are demonstrated in FPMC 2021 paper [5]. In that paper, the desired duty position, velocity, and acceleration trajectories were known beforehand but for the human-in-the-loop system, the references are generated in real-time.

The transition controller for discrete pressure rail switches is presented in [6] where the Least norm control formulation is described. It was assumed that the reference trajectories were available during the transition period for the Least Norm controller. The least norm controller minimizes the L2 norm of the control input and drives the system from the initial state to the final state in the presence of disturbance. The knowledge of the final state and the time course of the disturbances are required for computing the least norm solution for HHEA. For the human in the loop system, the pressure rail switches are modeled as a second-order filter with the knowledge of past and current rail selections. The velocity reference and the load force are assumed to be constant during the transition period as the transition period is short. The initial states are measured in real-time. The assumptions made enable the computation of the final states and the time course of disturbance to compute the least norm control input for all different switches.

5 Experimental testbed and results

The backhoe arm shown in Figure 3 is retrofitted with HHEA on the boom and stick actuator. The rod side of both the boom and stick actuators are connected to a hydraulic pump/motor and electric motor combination and the cap side of the actuators are connected to a 5-section Eaton CMA-90 valve. This combination forms the Hydraulic Electric Control Module

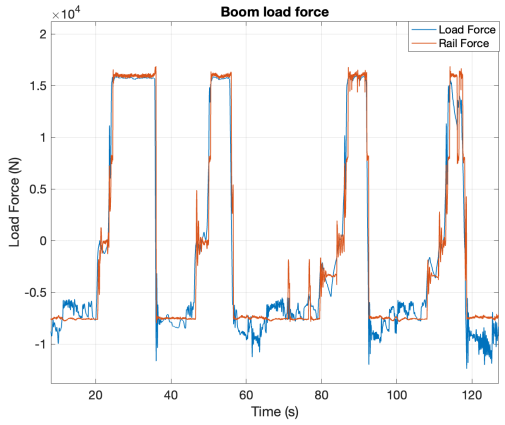

FIGURE 4. Load force vs Rail force with three pressure rails (50 bar, 25 bar, tank)

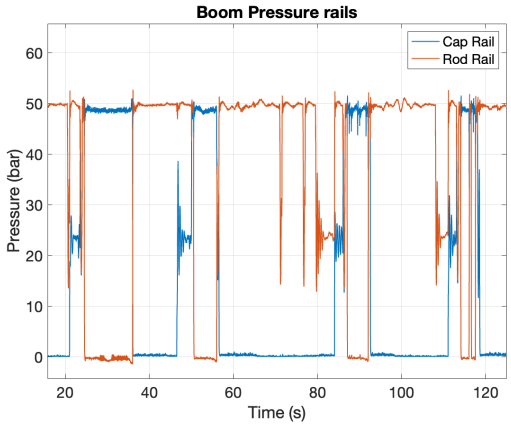

FIGURE 5. Pressure rails switches on the cap and rod side of the boom actuator

(HECM). The CMA valve is designed to serve two functions: switching pressure rails for both actuators and generating the middle-pressure rail (for the laboratory setup only). One of the work ports functions in pressure control mode to generate the middle-pressure rail, while the other four sections are operated in PWM mode to switch among three pressure rails on both the cap and rod ends of the two actuators. On an actual machine, the pressure rails will be generated efficiently by a pump. The external hydraulic power supply is responsible for generating both the high-pressure line and the tank line. A 10 cc Parker F-11 axial piston pump and a 5 kW electric motor by Clearpath Teknic are used in the boom HECM. A 3 cc gear pump and 1 kW electric motor by Clearpath Teknic are used for the stick's HECM. A two DOF analog joystick is used to control the motion of the stick and boom actuator.

5.1 Realtime switching results

The real-time pressure rail switching strategy discussed above is demonstrated on the backhoe testbed retrofitted with HHEA (Figure 3). In this experiment, the external loading on the boom actuator undergoes variation as the operator pushes the bucket against the ground, aiming to lift the backhoe frame off the ground.

In Figure 4 the load force acting on the boom cylinder is plotted with the pressure rail forces. As depicted in Figure 4, the load exerted on the boom actuator undergoes dynamic changes throughout the course of the experiment. Initially, before the bucket makes contact with the ground, the load on the boom actuator is solely due to the force of gravity. However, once the bucket hits the ground, a reaction load is generated, which acts on the boom cylinder. As the frame lifts off the ground, the load on the boom actuator eventually stabilizes and remains constant. The pressure rail switching strategy uses the pressure rail

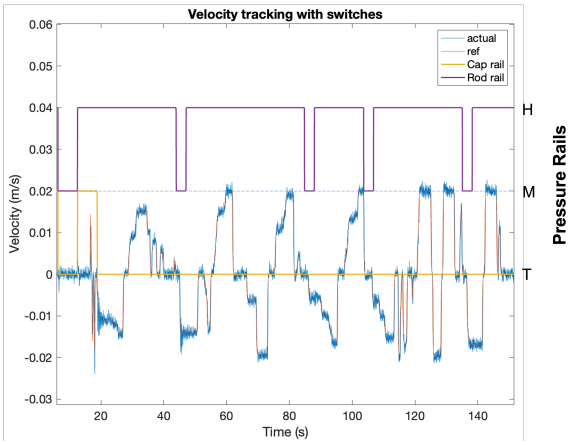

FIGURE 6. Velocity tracking for boom actuator in the presence of pressure rail switches

switches as shown in Figure 5 to provide the majority of the load force hydraulically. Overall, this experiment demonstrates the effectiveness of the real-time pressure rail switching strategy as the external load changes.

5.2 Reference tracking results

A separate experiment is carried out to assess the motion control performance of the backhoe in the presence of pressure rail switches with the control strategy discussed in Section 4. The backhoe arm's boom and stick actuators are controlled using a 2-degree-of-freedom (2-DOF) joystick, which establishes a velocity reference based on the joystick's position. The operator concurrently manipulates both the stick and boom actuators, while the real-time rail switching strategy triggers the pressure rail switches to accommodate changes in the load acting on these

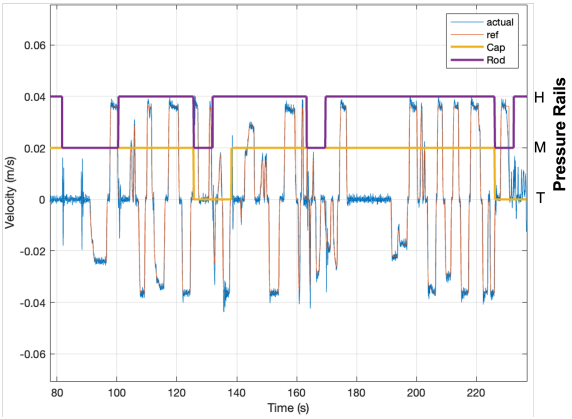

FIGURE 7. Velocity tracking for stick actuator in the presence of pressure rail switches

actuators. As depicted in Figure 6 and Figure 7, both the stick and boom actuators effectively track the reference velocity. The pressure rail selections made on both the cap and rod sides for each actuator are also shown. Notably, the impact of the switching process on the boom actuator is minimal due to its significant inertia, which inherently reduces velocity spikes during the switching events. The stick actuator which has a lower inertia, has more tracking errors during specific switches, resulting some velocity spikes. It is important to highlight that despite the slight tracking deviations and velocity spikes observed in the stick actuator during certain switches, the overall motion control algorithm and real-time pressure rail switching strategy employed for operating the backhoe yields excellent tracking performance for both the stick and boom actuators.

6 Human machine interface for intuitive operation

Skilled operators play a crucial role in ensuring the efficient and safe operation of off-road mobile machines, thereby impacting the productivity, quality, and safety of construction projects. However, the construction industry is currently facing a significant shortage of skilled laborers, posing challenges for construction companies in finding and hiring qualified operators. Acquiring a skilled operator can be both difficult and expensive.

Conventional human-machine interfaces for these machines use two 2-degree-of-freedom joysticks to control the four actuators (two for the arm and two for propel) independently. However, many tasks performed by these machines require the simultaneous utilization of multiple degrees of freedom, making precise operation a challenge that demands extensive practice.

To reduce the complexity of operating these machines so that even novice operators can effectively carry out required tasks without much training, we have developed several improvements to the human machine interface, on top of the HHEA trajectory control strategy described above to simplify machine operation.

6.1 Cartesian workspace operation

For a novice operator, it is more intuitive to perceive and conceptualize motion using Cartesian coordinates of the end effector. Thus, the 2D joystick motion is mapped to the Cartesian velocity of the bucket joint instead of the individual actuators.

Since the motion controller was developed in the actuator coordinates, a kinematic relationship is required to transform between the Cartesian workspace to the actuator space. If the forward kinematic relationship between the actuator strokes and the Cartesian coordinates of the bucket joint is $(X,Y) = f(q_1,q_2)$, then, the bucket joint's velocities and the actuator velocities are related via the Jacobian:

$$\begin{bmatrix}\dot{X}\\ \dot{Y}\end{bmatrix} = \underbrace{\frac{\partial f}{\partial q}(q_1,q_2)}_{J(q_1,q_2)}\begin{bmatrix}\dot{q}_1\\ \dot{q}_2\end{bmatrix} \tag{12}$$

Using (12), the velocity command in Cartesian coordinates can be easily converted into the velocity command in the actuator coordinates.

6.2 Pressure feedback design

The joystick control discussed so far is based solely on a velocity reference independent of the load that the machine experiences while attempting to track the reference. This can be dangerous to both the machine and its environment. One option is to use a haptic joystick to convey the load that the machine experiences via some form of haptic feedback. To assist the user to control the machine's physical interaction with its environment using only a simple, low-cost, non-haptic joystick, we incorporate force feedback into the generation of the reference velocity instead. The operator can decide to switch to this mode when required.

The main idea is that in the presence of an external load, the desired velocity is decreased. Let $q \in \Re^2$ be actuator space coordinates, and $x \in \Re^2$ be the workspace (end effector) coordinates. Suppose that the Cartesian velocity command based on joystick position alone is $v_{d,x}$. In the presence of external load (in Cartesian coordinates), F_x, the reference velocity is modified to be:

$$v_{ref,x}(t) = v_{d,x}(t) - \gamma \cdot F_x(t) \tag{13}$$

where γ is a positive gain. This causes the machine to naturally slow down when encountering external load. If the user desires to operate at a higher speed, he/she must work to increase the

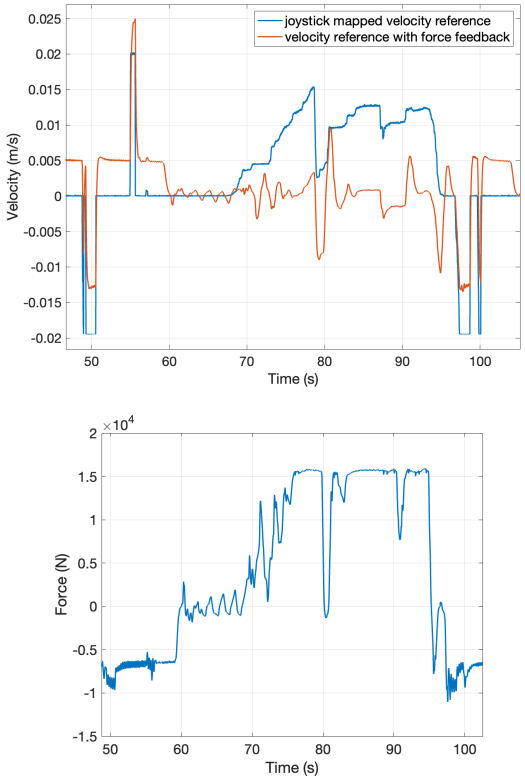

FIGURE 8. Velocity reference with force feedback and load force on boom actuator

command $v_{d,x}$. (13) can be expressed in the actuator coordinates as:

$$v_{ref,q} = J^{-1}(q)v_{d,x} - \gamma\left[J^{-1}(q)J^{-T}(q)\right]F_q \tag{14}$$

Here, we have utilized the Jacobian relationships between velocities and forces in the actuator coordinates and the Cartesian coordinates:

$$\dot{x} = J(q)\dot{q} \quad \dot{q} = J^{-1}(q)\dot{x}$$
$$F_q = J^T(q)F_x; \quad F_x = J^{-T}(q)F_q$$

(14) is implemented on the backhoe testbed where the backhoe arm is used to lift the body of the setup by pushing against the ground. Figure 8 compares the velocity reference with and without force feedback. It can be observed that as the load increases, the velocity reference with force feedback adapts to the load force and decreases the velocity, preventing the system from quickly moving up. This can help the operator to better interact with external forces.

6.3 Using velocity fields to specify tasks

Many tasks that off-road machines perform are quite repetitive. An example is a dig-lift-dump cycle. To assist novice operators to execute such tasks that normally require coordinating the motion of multiple actuators, the tasks can be encoded as velocity fields [10] [11]. By specifying a desired velocity at each possible machine position, a velocity field guides the machine to converge to the desired motion required for the task. Figure 9 is an example velocity field encoding the task of moving along a circle. Note that the arrows (the field) converge towards the circle. For other tasks, the motion can be provided by a skilled operator demonstrating how the task is performed. A velocity field can then be designed so that its limits converge to the captured motion.

The user can control this task with a two DOF joystick such that one DOF (up and down) controls the speed of operation; while the second DOF (left and right) controls how the machine should deviate from the nominal path specified by the velocity field.

To demonstrate this concept, we use the Cartesian space circular contour task as shown in Fig. 9. Let $v_f(q) \in \Re^2$ be velocity field for the task (i.e. as shown in Fig. 9) and $v_{fn}(q) \in \Re^2$ be a normal velocity field (not shown) such that the inner product between them is $\langle v_f(q), v_{fn}(q)\rangle = 0, \forall q$. The reference velocity to be tracked is defined to be:

$$v_{d,x} = \alpha(t)v_f(q) + \beta(t)v_{fn}(q) \tag{15}$$

where $\alpha(t)$ and $\beta(t)$ are the up-down and left-right joystick positions for scaling the nominal and normal velocity fields. In this way, the user needs only to move the joystick up and down ($\alpha(t)$) to control the speed of following the nominal circle. The coordination between different actuators is handled by the velocity field. If, on the other hand, the user needs to deviate from the nominal circle, then the user can move the joystick sideways ($\beta(t)$) to activate the normal field. This provides the operator full control over the machine.

Experimental results of the situation where the user only controls the speed are shown in Figure 10. Results when the user actively deviates from the nominal circle are shown in Figure 11.

7 Conclusions

The Hybrid Hydraulic Electric Architecture has been retrofitted to backhoe arm actuators, controlled by a 2-degree-of-freedom joystick operated by a human. The real-time switching strategy based on load force proximity to rail forces has been demonstrated. The motion control in the presence of pressure rail switches with a human operator controlling the backhoe boom and stick actuator has been shown. Experimental results demonstrate effective tracking performance even in the presence

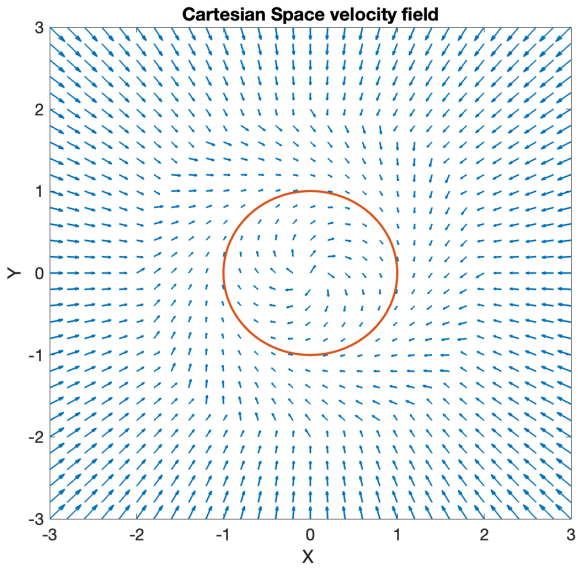

FIGURE 9. Velocity field for circular contour following task

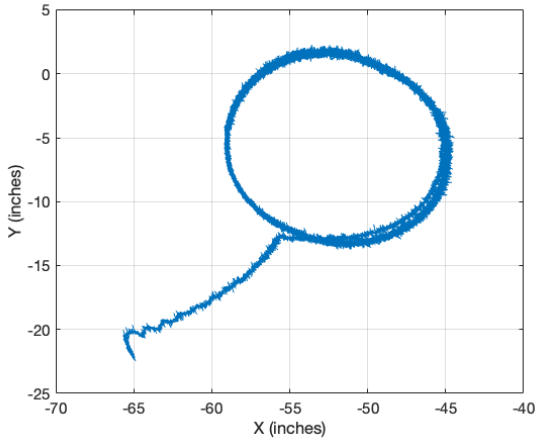

FIGURE 10. Backhoe arm following circular contour

of pressure rail switches. Efforts have been made to enhance the operation of mobile machines by modifying functions within the existing human-machine interface. An example of such progress is the implementation of velocity field control. This empowers novice operators to effortlessly adjust the rate of following a contour and make subtle trajectory adjustments, eliminating the need to coordinate multiple degrees of freedom. As a result, controlling tasks involving multiple degrees of freedom becomes simpler, enabling novice operators to perform them with minimized risks, heightened efficiency, and increased productivity.

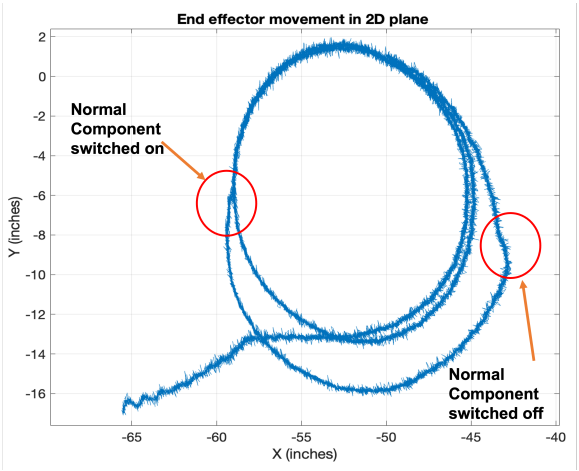

FIGURE 11. Deviation from a nominal contour

ACKNOWLEDGEMENTS

This material is based upon work supported by the Department of Energy, Office of Energy Efficiency and Renewable Energy (EERE) under the grant: EE0008384 and EE0009875. We are also grateful for component donations from Eaton, Danfoss, and Parker Hannifin.

REFERENCES

[1] L. Love, E. Lanke, and P. Alles, "Estimating the impact (energy, emissions and economics) of the us fluid power industry," *Oak Ridge National Laboratory (ORNL), TN*, no. ORNL/TM-2011/14, 2012.

[2] P. Y. Li, J. Siefert, and D. Bigelow, "A hybrid hydraulic-electric architecture (HHEA) for high power off-road mobile machines," in *BATH/ASME 2019 Symposium on Fluid Power and Motion Control*. American Society of Mechanical Engineers, 2019.

[3] J. Siefert and P. Y. Li, "Optimal control and energy-saving analysis of common pressure rail architectures: Hhea and steam," in *BATH/ASME 2020 Symposium on Fluid Power and Motion Control*. American Society of Mechanical Engineers Digital Collection, 2020.

[4] ——, "Optimal control and energy-saving analysis of common pressure rail architectures: Hhea and steam," vol. BATH/ASME 2020 Symposium on Fluid Power and Motion Control, 09 2020, v001T01A050. [Online]. Available: https://doi.org/10.1115/FPMC2020-2799

[5] A. Chatterjee and P. Y. Li, "Hil testbed and motion control strategy for the hybrid hydraulic electric architecture (hhea)," in *ASME/BATH 2021 Symposium on Fluid Power and Motion Control*, 2022.

[6] ——, "Motion control of hydraulic actuators in the presence of discrete pressure rail switching," in *2020*

IEEE/ASME International Conference on Advanced Intelligent Mechatronics (AIM), 2020, pp. 1956–1961.

[7] J. Siefert and P. Y. Li, "Optimal control of the energy-saving hybrid hydraulic-electric architecture (hhea) for off-highway mobile machines," *IEEE Transactions on Control Systems Technology*, vol. 30, no. 5, pp. 2018–2029, 2022.

[8] ——, "Optimal operation of a hybrid hydraulic electric architecture (hhea) for off-road vehicles over discrete operating decisions," in *2020 American Control Conference (ACC)*, 2020, pp. 3255–3260.

[9] A. Khandekar, J. Wills, M. R. Wang, and P. Y. Li, "Incorporating valve switching losses into a static optimal control algorithm for the hybrid hydraulic-electric architecture (HHEA)," in *ASME/BATH 2021 Symposium on Fluid Power and Motion Control*, 2021, v001T01A046. [Online]. Available: https://doi.org/10.1115/FPMC2021-69045

[10] P. Y. Li and R. Horowitz, "Passive velocity field control of mechanical manipulators," *Robotics and Automation, IEEE Transactions on*, vol. 15, no. 4, pp. 751–763, 1999.

[11] P. Li and R. Horowitz, "Passive velocity field control (pvfc). part ii. application to contour following," *IEEE Transactions on Automatic Control*, vol. 46, no. 9, pp. 1360–1371, 2001.